C, N and P stoichiometric mismatch between resources and consumers influence the dynamics of a marine microbial food web model and its response to atmospheric N and P inputs

Philippe Pondaven, Pascal Rivière, Céline Ridame, Cécile Guieu

Biogeosciences Discuss., 11, 2933–2971, 2014
www.biogeosciences-discuss.net/11/2933/2014/
doi:10.5194/bgd-11-2933-2014

Biogeosciences Discussions
Open Access

C, N and P stoichiometric mismatch between resources and consumers influence the dynamics of a marine microbial food web model and its response to atmospheric N and P inputs

P. Pondaven[1], P. Pivière[1], C. Ridame[2,3], and C. Guien[4,5]

[1]Université de Brest; Institut Universitaire Européen de la Mer, IUEM; Laboratoire des Sciences de l'Environnement Marin, UMR 6539 LEMAR, Technopôle Brest Iroise, Place Nicolas Copernic, 29280 Plouzané, France
[2]CNRS-INSU/IRD/MNHN/UPMC, UMR 7159, LOCEAN, Laboratoire d'Océanographie et du Climat: Expérimentation et Approches Numériques, 75252, Paris, France
[3]Sorbonne Universités, UPMC Univ Paris 06, UMR 7159, LOCEAN, 75252 Paris, France
[4]Sorbonne Universités, UPMC Univ Paris 06, UMR 7093, LOV, Observatoire océanologique, 06230, Villefranche/mer, France
[5]CNRS, UMR 7093, LOV, Observatoire océanologique, 06230, Villefranche/mer, France

Received: 23 December 2013 – Accepted: 10 January 2014 – Published: 20 February 2014

Correspondence to: P. Pondaven (philippe.pondaven@univ-brest.fr)

Published by Copernicus Publications on behalf of the European Geosciences Union.

Abstract

Results from the DUNE experiments reported in this issue have shown that nutrient input from dust deposition in large mesocosms deployed in the western Mediterranean induced a response of the microbial food web, with an increase of primary production rates (PP), bacterial respiration rates (BR), as well as autotrophic and heterotrophic biomasses. Additionally, it was found that nutrient inputs strengthened the net heterotrophy of the system, with NPP : BR ratios < 1. In this study we used a simple microbial food web model, inspired from previous modelling studies, to explore how C, N and P stoichiometric mismatch between producers and consumers along the food chain can influence the dynamics and the trophic status of the ecosystem. Attention was paid to the mechanisms involved in the balance between net autotrophy vs. net heterotrophy. Although the model was kept simple, predicted changes in biomass and PP were qualitatively consistent with observations from DUNE experiments. Additionally, the model shed light on how ecological stoichiometric mismatch between producers and consumers can control food web dynamics and drive the system toward net heterotrophy. In the model, net heterotrophy was notably driven by the parameterisation of the production and excretion of extra DOC from phytoplankton under nutrient-limited conditions. This mechanism yielded to high C : P and C : N ratios of the DOM pool, and subsequent postabsorptive respiration of C by bacteria. The model also predicted that nutrient inputs from dust strengthened the net heterotrophy of the system; a pattern also observed during two of the three DUNE experiments (P and Q). However, the model was not able to account for the low NPP : BR ratios (down to 0.1) recorded during the DUNE experiments. Possible mechanisms involved in this discrepancy were discussed.

BGD
11, 2933–2971, 2014

1 Introduction

The Mediterranean Sea is a typical oligotrophic sea (Siokou-Frangou et al., 2010), where the growth rate of autotrophic and heterotrophic osmotrophs is limited by the availability of macro and/or micronutrients, notably phosphorus (Thingstad et al., 1998, 2005; Pinhassi et al., 2006; Tanaka et al., 2011), and at specific moments, possibly iron (Bonnet et al., 2005). In this context, atmospheric deposition of Saharan dust can be a major source of nutrients to the surface of the Mediterranean Sea in particular during stratification periods (see for ex. Bergametti et al., 1992; Ternon et al., 2011). The question of how these dust events influence microbial food webs has been investigated in recent years using microcosm experiments fertilised with natural or processed aeolian dust (Zohary et al., 2005; Herut et al., 2005). In dust addition experiments, the magnitude of the biological response to dust deposition has been shown to depend on the degree of oligotrophy where dust deposition occurs (Marañón et al., 2010). In this issue Guieu et al. (2014a) describe results from a set of large mesocosm experiments deployed at an oligotrophic coastal site in the northwestern (NW) Mediterranean Sea (DUNE project: "a DUst experiment in a low-Nutrient, low chlorophyll Ecosystem"). During these experiments, realistic simulations of dust deposition were performed in 52 m^3 cleaned bags (Guieu et al., 2014a). The waters enclosed in mesocosms before dust deposition were typically oligotrophic, with low chlorophyll biomass (50–140 $ng\,L^{-1}$; Ridame et al., 2014), low concentration of Dissolved Inorganic Phosphorus (DIP) (4 ± 1 nM-P, Pulido-Villena et al., 2010, 2013) and Nitrogen (DIN) (< 30 nM-N; Ridame et al., 2014), and concentrations of iron (Fe) ranging from 2.2 nM-Fe to 4.4 nM-Fe (Wuttig et al., 2013). These Fe concentrations were thought to be unlimiting for phytoplankton growth, owing to the low Fe half-saturation constants for growth usually reported in the literature (Price et al., 1994; Timmermans et al., 2004). The simulated dust event induced a transient increase in the concentrations of macro nutrients, which in turn stimulated, to different degrees, microbial activity (Pulido-Villena et al., 2014; Giovagnetti et al., 2013; Guieu et al., 2014b; Ridame et al., 2013; 2014).

BGD
11, 2933–2971, 2014

The mechanisms by which nutrient addition has affected key ecological processes – such as the balance between net autotrophy and net heterotrophy, remain discussed (Guieu et al., 2014b). The magnitude of the ecosystem response to nutrient addition has at least two components: (1) nutrient input from dust directly relieved producers from chronic substrate limitation; (2) stoichiometric constrains within the food web result in differential Consumer-driven Nutrient Recycling (CNR), which in turn feedbacks on osmotrophic producers (Sterner and Elser, 2002).

Here we present a model focusing on this second mechanism. Ecological stoichiometry provides experimental and theoretical insights on the mechanisms involved in CNR. The basic principles of this theory suggest that a mismatch between the elemental composition of producers and consumers, coupled with homeostatic regulation of the elemental composition in consumers, result in differential assimilation and excretion of chemical elements (Sterner and Elser, 2002). As a consequence, the elemental stoichiometry of nutrient excretion from consumers (called "resupply ratio", Sterner, 1990) varies, depending on food elemental composition. In turn variations in nutrient resupply ratios can change the balance of the limiting elements in the environment (Boersma et al., 2008). Until recently this hypothesis considered mainly pairwise interactions between autotrophic organisms and herbivores (Sterner, 1990; Daufresne and Loreau, 2001), but more recent studies have highlighted the role of bacterial decomposers in driving CNR (Danger et al., 2007; Cherif and Loreau, 2008).

Several reasons suggest that stoichiometric constrains within food web can influence the response of marine microbial food webs to nutrient addition from dust. First, there are accumulating evidences that nutrient cycling mediated by consumers could determine the limiting nutrient for producer growth in the ocean (Le Borgne, 1982; Hjerne and Hansson, 2002; Steinberg et al., 2008; Pitt et al., 2009; Nugraha et al., 2010). Second, natural mortality rates of small marine prokaryotes and eukaryotes are primarily driven by either viral lysis or grazing (Calbet, 2001; Landry and Calbet, 2004), which results in a rapid turnover of chemical elements at the surface of the ocean.

BGD
11, 2933–2971, 2014

The model described herein was admittedly kept simple compared to more realistic stoichiometric models (e.g., Touratier et al., 2001; Anderson et al., 2005). It used a classic mass balance approach to calculate C, N, and P gross growth efficiency (GGE) for consumers which feed on different types (in term of quality) of preys. Model simulations were qualitatively compared with existing observations from DUNE experiments, but no attempt was made to optimise the model to fit the observations. The aim of this study was rather to construct a stoichiometric model as supportive material to assess whether C, N and P stoichiometric mismatch between producers and consumers can influence the dynamics and the trophic status of a microbial food web. For this purpose we compared the behaviour of the model, before and after dust seeding, for different scenarios which only differ by the strength of the stoichiometric mismatch between producers and consumers.

2 Model description

2.1 Model framework

The conceptual scheme of the microbial food web model is based on Thingstad et al. (2007; Fig. 1). It includes three osmotrophs: heterotrophic bacteria (B_P), and two phytoplankton types, picoautotrophs (A_P) and nanoautotrophs (D_P). The growth rate of phytoplankton relies on the availability of dissolved inorganic nitrogen (N_i) and phosphorus (P_i). Bacterial growth primarily relies on the availability of dissolved organic matter (DOM), and secondarily on the availability of N_i and P_i, when the N : C or the P : C ratio of DOM is low compared to bacterial requirement (Anderson and Williams, 1998). Three predators are included in the model: heterotrophic nanoflagellates (H_P), ciliates (C_P) and mesozooplankton (M_P). Heterotrophic nanoflagellates feed on bacteria and picoautotrophs, ciliates feed on heterotrophic nanoflagellates, and nanoautotrophs, and mesozooplankton feed on ciliates and nanoautotrophs. The subscript "P" indicates that the main model currency is phosphorus. It is assumed that all organisms

BGD
11, 2933–2971, 2014

have a fixed C : N : P elemental composition, so that explicit equations for N and C pools are not required, excepted for DOM and inorganic nutrient concentrations.

2.2 Model formulation

The system of differential equations describing trophic interactions and the fate of C, N and P are given in Table 1. Model parameters and their values are listed in Table 2. The mathematical formulations of the biological processes were described below.

2.2.1 Phytoplankton growth rates

The growth rates of pico autotrophs (U_{pico}, h^{-1}) and nano autotrophs (U_{nano}, h^{-1}) depended on the external concentration of dissolved inorganic N and dissolved inorganic P, using a Liebig's Law formulation:

$$U_{\text{pico}} = \mu_{\text{max}}^{\text{pico}} \min\left[\frac{P_i}{P_i + K_{P_i}^{\text{Pico}}}, \frac{N_i}{N_i + K_{N_i}^{\text{Pico}}}\right]$$

and,

$$U_{\text{nano}} = \mu_{\text{max}}^{\text{nano}} \min\left[\frac{P_i}{P_i + K_{P_i}^{\text{nano}}}, \frac{N_i}{N_i + K_{N_i}^{\text{nano}}}\right]$$

Picoplankton has a higher maximal growth rate and a higher affinity (i.e. lower $K_{N_i}^{\text{pico}}$ and $K_{P_i}^{\text{pico}}$) compared to nanophytoplankton (Table 2). Light was supposed to be unlimiting in the mesocosms.

2.2.2 Loss rates from predation

Grazing rate of consumer "k" feeding on prey "j", I_j^k (h^{-1}), were parameterised according to Gismervik and Andersen (1997). For examples, grazing rates of ciliates (C_P) on

BGD
11, 2933–2971, 2014

nanoautotrophs (D_P) and heterotrophic nanoflagellates (H_P) were written:

$$I_D^C = g_C^{max} \frac{(D_P/C_D^C)^{\varphi}}{\left(1 + \left(D_P/C_D^C\right)^{\varphi} + \left(H_P/C_H^C\right)^{\varphi}\right)},$$

and,

$$I_H^C = g_C^{max} \frac{(H_P/C_H^C)^{\varphi}}{\left(1 + \left(D_P/C_D^C\right)^{\varphi} + \left(H_P/C_H^C\right)^{\varphi}\right)}$$

Where g_C^{max} was the maximal grazing rate (h^{-1}), C_i^j were the incipient limiting prey concentrations, and φ was the switching shape parameter. Here, φ was set to 2.0, which corresponds to a type 3 functional response (Gismervik and Andersen, 1997).

2.2.3 Gross Growth Efficiency, GGE, and homeostatic regulation of C, N, and P elemental composition in heterotrophic organisms

Homeostatic regulation of whole body elemental composition in a consumer is maintained by releasing elements which are in excess to requirements, while more efficiently retaining limiting elements. Thus, when a consumer feeds on preys with variable elemental composition, the gross growth efficiency (GGE) will differ between elements to maintain homeostasis (Sterner and Elser, 2002). In this study we used a simple mass balance approach to calculate GGE. In the model, GGE was called a_i^{jk} (with i = C, N or P, for a consumer k feeding on a prey j). Considering the three elements C, N and P, homeostatic regulation of the C : P and C : N ratio in a consumer k feeding on a prey j was verified if:

$$\theta_j^{CP} \frac{a_C^{jk}}{a_P^{jk}} = \theta_k^{CP},$$

BGD
11, 2933–2971, 2014

and,

$$\theta_j^{\mathrm{CN}} \frac{a_{\mathrm{C}}^{jk}}{a_{\mathrm{N}}^{jk}} = \theta_k^{\mathrm{CN}}$$

Where θ_j^{CP}, θ_k^{CP}, θ_j^{CN} and θ_k^{CN}were the C : P and C : N ratios of prey j and consumer k, and a_{C}^{jk}, a_{N}^{jk} and a_{P}^{jk}, were the GGE for C, N and P, respectively. This system of two linear equations has three unknowns (a_{C}^{jk}, a_{N}^{jk} and a_{P}^{jk}), accepting an infinite number of possible solutions (Fig. 2). However, in a context where individuals compete for resource, natural selection would favour a "strategy" (solution) which maximises GGE for each element, while at the same time maintaining a fixed elemental in the consumer. These optimal solutions for a_{C}^{jk}, a_{N}^{jk} and a_{P}^{jk} were (Fig. 1):

$$a_{\mathrm{C}}^{jk} = \min\left[a_i^{\max}, a_i^{\max}\theta_k^{\mathrm{CP}}/\theta_j^{\mathrm{CP}}, a_i^{\max}\theta_k^{\mathrm{CN}}/\theta_j^{\mathrm{CN}}\right]$$

$$a_{\mathrm{N}}^{jk} = a_{\mathrm{C}}^{jk}\theta_j^{\mathrm{CN}}\left(\theta_k^{\mathrm{CN}}\right)^{-1}$$

$$a_{\mathrm{P}}^{jk} = a_{\mathrm{C}}^{jk}\theta_j^{\mathrm{CP}}\left(\theta_k^{\mathrm{CP}}\right)^{-1}$$

For example, for a prey j and a predator k with: $\theta_j^{\mathrm{CP}} = 100$, $\theta_k^{\mathrm{CP}} = 150$, $\theta_j^{\mathrm{CN}} = 11$ and $\theta_k^{\mathrm{CN}} = 6$, it can be verified (assuming that $a_i^{\max} = 0.90$):

$$a_{\mathrm{C}}^{jk} = \min\left[1, 1 \times 150/100, 1 \times 6/11\right] = 0.49091,$$

$$a_{\mathrm{N}}^{jk} = a_{\mathrm{C}}^{jk} \times \left(11 \times (6)^{-1}\right) = 0.90, \text{ and,}$$

$$a_{\mathrm{P}}^{jk} = a_{\mathrm{C}}^{jk} \times \left(100 \times (150)^{-1}\right) = 0.32727,$$

BGD
11, 2933–2971, 2014

In this case, food would be primarily N-limited, and secondarily C-limited. These solutions also maintain strict homeostasis of C, N and P elemental composition for the consumer:

$$\theta_j^{\mathrm{CP}} \frac{a_{\mathrm{C}}^{jk}}{a_{\mathrm{P}}^{jk}} = \theta_k^{\mathrm{CP}}, \text{ i.e.} 100 \times \frac{0.49091}{0.32727} = 150$$

and,

$$\theta_j^{\mathrm{CN}} \frac{a_{\mathrm{C}}^{jk}}{a_{\mathrm{N}}^{jk}} = \theta_k^{\mathrm{CN}}, \text{ i.e.} 11 \times \frac{0.49091}{0.90} = 6$$

This formulation can be extended to more than three elements. In the model we used a maximal accumulation efficiency of $a_i^{\max} = 0.75$ (e.g. Sterner, 1990; Straile, 1997).

Bacteria differ from the other heterotrophic organisms (heterotrophic nanoflagellates, ciliates and mesozooplankton), because C, N or P imbalance in food compared to requirement can be partly compensated by inorganic nutrient uptake. To account for this process, parameterisation of bacterial growth, excretion, and respiration follows Anderson and Williams (1998) model. This model assumes that dissolved organic matter is the primary growth substrates (here L_{DOC}, L_{DON} and L_{DOP}), with dissolved inorganic nitrogen ($\mathrm{N_i}$) or phosphorus ($\mathrm{P_i}$) supplementing DOM when the C : N and/or the C : P ratio of DOM is high.

BGD
11, 2933–2971, 2014

Uptake rates of L_{DOC} (U_B^{DOC}), L_{DON} (U_B^{DON}) and L_{DOP} (U_B^{DOP}), and the potential uptake of dissolved inorganic nitrogen ($U_B^{N_i}$) and phosphorus ($U_B^{P_i}$) were written:

$$U_B^{DOC} = \frac{\mu_B^{max} L_{DOC}}{L_{DOC} + K_{LDOC}} \theta_B^{CP} B_P$$

$$U_B^{DON} = U_B^{DOC} \frac{L_{DON}}{L_{DOC}}$$

$$U_B^{DOP} = U_B^{DOC} \frac{L_{DOP}}{L_{DOC}}$$

$$U_B^{N_i} = \frac{\mu_B^{max} N_i}{N_i + K_{N_i}} \theta_B^{NP} B_P$$

$$U_B^{P_i} = \frac{\mu_B^{max} P_i}{P_i + K_{P_i}} B_P$$

The potential bacterial excretion of inorganic N (E_B^N) or inorganic P (E_B^N) were written:

$$E_B^N = U_B^{DON} - \omega_B U_B^{DOC} \theta_B^{NC}$$

and

$$E_B^P = U_B^{DOP} - \omega_B U_B^{DOC} \theta_B^{PC},$$

In these equations, ω_B represented the maximal GGE. If $E_B^N > 0$ and/or $E_B^P > 0$, N and/or P were in excess to requirement in DOM. In this case, there was no need for extra N or P uptake from the dissolved inorganic pool (i.e. $U_B^{N_i} = 0$, or $U_B^{P_i} = 0$), and bacterial excretion of N or P were equal to E_B^N or E_B^P.

Conversely, if $E_B^N < 0$ and/or $E_B^P < 0$, N and/or P were in deficit to requirement in DOM. Then bacterial N or P requirement will be fulfilled by inorganic N or P uptake. In this case, there were two possibilities:

BGD
11, 2933–2971, 2014

1. When potential inorganic N or P uptake is insufficient to meet demand ($E_B^N < 0$, and $-E_B^N > U_B^{N_i}$, or $E_B^P < 0$, and $-E_B^P > U_B^{P_i}$), total N (or P) uptake was equal to $U_B^{DON} + U_B^{N_i}$ (or $U_B^{DOP} + U_B^{P_i}$ for P), and the excess of carbon found in DOM was respired (E_C^B), that is: $E_C^B = U_B^{DOC} - \theta_B^{CN}\left(U_B^{DON} + U_B^{N_i}\right)$.

2. When potential inorganic N or P uptake was sufficient to meet demand ($E_B^N < 0$, and $-E_B^N < U_B^{N_i}$, or $E_B^P < 0$, and $-E_B^P < U_B^{P_i}$), then $U_B^{N_i} = -E_B^N$ (or $U_B^{P_i} = -E_B^P$ for P), and respiration, $E_C^B = (1 - \omega_B) U_B^{DOC}$.

2.2.4 Other processes

Production from L_{DOC} from phytoplankton exudation, E_P, was directly proportional (parameter δ_P) to primary production (Anderson and Pondaven, 2003):

$$E_P = \delta_P \left(U_A\, A_P \theta_A^{CP} + U_D D_P \theta_D^{CP}\right)$$

Finally, E_{P_i} and E_{N_i} represented the external source of dissolved inorganic nutrients (here from experimental dust deposition). E_{P_i} and E_{N_i} were set to 0 in the control simulation. In this case, the model solution reached a stable steady state (see model results).

In the model, mesozooplankton represented the highest trophic level, and the model used a linear mortality term for this variable ($\delta_M M_p$, Table 1) to account for both predation and mortality due to aging.

Non-assimilated products and detritus coming from mesozooplankton mortality returned to the dissolved inorganic or organic nutrient pools. The parameter λ_e (dimensionless) represented the proportion of these waste products and detritus that went to the dissolved inorganic pool, or respired CO_2; $(1 - \lambda_e)$ going to the dissolved organic pool.

BGD
11, 2933–2971, 2014

The steady state solutions from the control simulation were then used as starting conditions for the simulation with nutrient addition from dust. In the model, the dust was added to the mesocosms at start (t0) with one single spike. The transient behaviour of the model was studied after dust seeding for each case. The inorganic nutrient input at time t0 corresponded to the average nutrient input during DUNE experiments (Ridame et al., 2014), i.e. 4.3 nmol-P L^{-1} and 498 nmol-N L^{-1}; assuming that only 35 % of total P dissolved (Pulido-Villena et al., 2010), and considering, as a first approximation, an homogeneous dilution of the particules releasing the nutrient.

2.2.5 Evaluating the influence of stoichiometric mismatch on food-web dynamics

The influence of stoichiometric mismatch on food web dynamics was explored by comparing model results from 1000 simulations in which the carbon, nitrogen and phosphorus elemental stoichiometry of each organism was chosen randomly in a range of ±50 % around the Redfield ratio (C : N : P = 106 : 16 : 1; the other parameters were set to their default values given in Table 2). These 1000 simulations accounted for different cases, i.e. from a "weak stoichiometric mismatch" (all resources and their consumers had similar C : N : P elemental compositions), to a "strong stoichiometric mismatch" (resources and consumers had distinct C : N : P elemental compositions). Then, for each simulation, we defined an index of C : P and C : N stoichiometric mismatch, $I_{C:P}$ and $I_{C:N}$, respectively:

$$I_{C:P} = \sum_{i=1}^{i=n} \left[\left(\theta_j^{CP} - \theta_k^{CP} \right) \frac{F_{jk}^i}{F_T^i} \right]$$

and

$$I_{C:N} = \sum_{i=1}^{i=n} \left[\left(\theta_j^{CN} - \theta_k^{CN} \right) \frac{F_{jk}^i}{F_T^i} \right]$$

BGD
11, 2933–2971, 2014

where "i" represented a particular resource-consumer interaction. In the model, seven distinct resource-consumer interactions were considered: DOM → Bp, Bp → Hp, Ap → Hp, Dp → Cp, Dp → Mp, Hp → Cp, and Cp → Mp (Fig. 1). θ_{ji}^{CP}, θ_{ki}^{CP}, θ_{ji}^{CN}, θ_{ki}^{CN} were the C : P or C : N ratios of the resource or prey "j" and the consumer "k". Finally the ratio F_{jk}^{i}/F_{T}^{i} represented the contribution of the consumption of resource or prey "j" by consumer "k" (nM-P d^{-1}) to the total daily ration of consumer "k" (all resources or preys combined). The F_{jk}^{i}/F_{T}^{i} ratio was equal to 1 if the consumer was a specialist feeding on a single resource or prey.

When $I_{C:P}$ or $I_{C:N} < 0$, this characterised the first type of mismatch with an excess of phosphorus or nitrogen – and a deficit of carbon – in the resources compared to consumer's requirements. Conversely, when $I_{C:P}$ or $I_{C:N} > 0$, this characterised the second type of mismatch with a deficit of phosphorus or nitrogen – and an excess of carbon – in the resources compared to consumer's requirements. When $I_{C:P} \to 0$ and $I_{C:N} \to 0$, resources and consumers had similar C : N : P elemental compositions (no mismatch).

3 Results

3.1 Intrinsic ecosystem dynamics

The intrinsic ecosystem dynamics was studied before performing the analysis of how stoichiometric mismatch influence the food web dynamics and the ecosystem response to nutrient addition. The objective was to characterise the sensitivity of the modelled system to variations of the total amount of nutrients available at time $t = 0$ (N_0 for nitrogen and P_0 for phosphorus). Sensitivity to model parameters was also studied. Model sensitivity was evaluated, numerically, by looking at the asymptotic behaviour of the system as t→ ∞, using a range of possible values for N_0, P_0, and the other model parameters.

BGD
11, 2933–2971, 2014

For this sensitivity analysis, variations of N_0 and P_0 and variations of the other model parameters were treated separately: (a) in a first part, the intrinsic ecosystem dynamics was explored in the N_0-P_0 parameter space (with the other model parameters set to their default values, Table 2). (b) In a second part, N_0 and P_0 were set to their values observed in the control experiment during the DUNE experiments (Ridame et al., 2014), and a series of 1000 different model simulations were performed, where all the other model parameters were chosen randomly in a range of ±50 % around their default values listed in Table 2.

The main conclusions from this sensitivity analysis are summarised below:

(a) Whatever the values for N_0 (in the range 1–10 000 nM-N) or P_0 (in the range 1–1000 nM-P), model solutions converged on fixed points as $t \rightarrow \infty$ for all state variables (Supplement S1). Also, the ecosystem structure was not affected by changes of both N_0 and P_0: all organisms coexisted in the N_0-P_0 parameter space; only the relative dominances were modified. These results were mainly driven by:

(a1) The conceptual scheme of the food web model which, with three predator populations (heterotrophic nanoflagellates, ciliates and mesozooplankton), resulted in selective predation which allowed to maintain coexistence between three groups of osmotroph competitors (bacteria, autotrophic pico- and nanoplankton) (Thingstad et al., 2007).

(a2) Model parameterisation of predator-prey interactions (Type III functional response) which tends to stabilise the system (see paragraph (b) below).

(b) The simulations where the model parameters were chosen randomly (in a range of ±50 % around their default values) – while N_0 and P_0 were fixed – showed that the asymptotic model solutions as $t \rightarrow \infty$ changed from fixed points to limit cycles (not shown). However, it was observed that limit cycles emerged when the switching shape parameter for the functional response $\varphi \rightarrow 1$ (type II functional response). Conversely, limit cycles disappeared when $\varphi \rightarrow 2$, (i.e. the default value defining a type III functional response).

BGD
11, 2933–2971, 2014

In summary, the food web model described here was relatively robust to perturbations. It should be noted that model simulations presented hereafter were performed using $\varphi = 2$, and the parameters listed in Table 2.

3.2 Influence of stoichiometric mismatch on food-web dynamics

The influence of stoichiometric mismatch on the ecosystem dynamics was explored as detailed in the method section (Sect. 2.2.5). Thus, Figs. 2–5 described model results from 1000 simulations where the carbon, nitrogen and phosphorus elemental stoichiometry of each organism was chosen randomly in a range of ±50 % around the Redfield ratio, which represented a range of values which can be recorded in the ocean.

3.2.1 Food-web dynamics

Variations of the C : N : P elemental composition of each organism induced changes in the relative dominance of predators and osmotrophs. These changes were driven by a classical trophic cascade mechanism (Fig. 2). Predators exerted a negative feedback on their preys (Fig. 2a, b, and d), with one exception: mesozooplankton and nanophytoplankton (Fig. 2d). However, this exception was also explained by a trophic cascade mechanism: mesozooplankton fed on ciliates which were the main consumers of nanophytoplankton in the model. As a consequence, when mesozooplankton biomass increased, nanophytoplankton was relieved from ciliates grazing pressure. For the same reason, the increase in mesozooplankton biomass had a positive feedback on HNF (Fig. 2e). Similarly, ciliates had a positive feedback on picophytoplankton and bacteria (Fig. 2e) by relieving these organisms from HNF grazing pressure (Fig. 2a). Finally mesozooplankton had a negative feedback on HNF preys (bacteria and picophytoplankton, Fig. 2f) by relieving HNF from ciliates predation.

BGD
11, 2933–2971, 2014

3.2.2 Influences of stoichiometric mismatch on primary production and respiration

All other things being equal, changes in the C : N : P elemental composition of organisms induced variations of primary production (PP which did not take into accounted the production and release of dissolved organic carbon; parameter δ_P, Table 2) and community respiration (CR) by a factor of 2.6 nM-P d^{-1} and 3.6 µg C L^{-1} d^{-1}, respectively. Thus, PP increased (Fig. 3a), while CR decreased (Fig. 3b), when the index of C : P stoichiometric mismatch, $I_{C:P}$, decreased. Conversely, only CR, and not PP, was significantly correlated to the index of C : N stoichiometric mismatch, $I_{C:N}$, ($r^2 = 0.41$, $p < 0.01$; not shown).

As mentioned previously, lower $I_{C:P}$ or $I_{C:N}$ characterised an excess of phosphorus or nitrogen in food compared to consumer's requirement, yielding to postabsorptive excretion of DIP and DIN from consumers. Figure 4a shows that PP was significantly correlated to DIP excretion, while it was not correlated to DIN excretion (Fig. 4b), demonstrating that PP was P-limited in the model.

Combining the 1000 simulations, the predicted average PP was 3.32 ± 0.77 µg C L^{-1} d^{-1} (± one Standard Deviation, SD) and CR was 3.55 ± 0.95 µg C L^{-1} d^{-1}. For PP, the model was consistent with observations from the control bags when considering all the DUNE experiments (PP = 4.6± 1.1 µg C L^{-1} d^{-1}; Guieu et al., 2014b). For BR however, the model underestimated the observed respiration rates, with bacterial respiration (BR) largely exceeding PP (BR = 19.3 ± 13.0 µg C L^{-1} d^{-1} in the control mesocosms when considering all the DUNE experiments; Guieu et al., 2014b). For comparison, the model predicted an average BR of 1.64 ± 0.38 µg C L^{-1} d^{-1}. Possible reasons for this discrepancy are commented in the discussion.

The model also predicted a shift from net autotrophy to net heterotrophy along the gradient of C : P and C : N stoichiometric mismatch (Fig. 5); net autotrophy vs. net heterotrophy was calculated from the ratio between gross PP (GPP) and CR. This shift was consistent with the fact that higher $I_{C:P}$ and $I_{C:N}$ characterised a carbon excess in

BGD
11, 2933–2971, 2014

food compared to consumer's requirement, which resulted in higher carbon dissipation from consumers (through respiration). As mentioned above, the model was however not able to predict the low Net PP : BR ratios recorded during the DUNE experiments (Guieu et al., 2014b).

3.2.3 Influences of stoichiometric mismatch on the ecosystem response to nutrient input from dust

To evaluate the influence of stoichiometric mismatch on the ecosystem response to N and P inputs from dust, three contrasting scenarios for the C : N : P elemental composition of organisms were selected from the 1000 simulations described in the previous section: i.e. the scenarios with C : N : P ratios which yielded to (1) the lowest $I_{C:P}$ (P excess in food), (2) $I_{C:P} \sim 0$ (no mismatch), and (3) the highest $I_{C:P}$ (C excess in food). Two additional cases were treated: (4) C : N : P elemental compositions following Redfield (1963) for all organisms, and (5) C : N : P elemental compositions recorded in a pristine lagoon on the west coast of central Norway (Vadstein et al., 2012; i.e. a study in which the elemental stoichiometry of all trophic groups was studied simultaneously). Table 3 listed the C : N : P elemental compositions used for each scenario. For each scenario, initial conditions (before nutrient addition from dust) were the asymptotic model solutions at time $t = 4 \times 10^4$ h (Fig. 2).

One single nutrient dust deposition was simulated, by adding +4.30 nM-P and +498 nM-N at time $t = 0$ (i.e. the mean from DUNE experiments, Ridame et al., 2014). Following simulated N and P nutrient input, DIP and DIN concentrations rapidly decreased (Fig. 6a and b), while primary production and respiration increased (Fig. 7a and b). The DIN : DIP ratios slightly increased for all scenarios, excepted for the scenario in which $I_{C:P} \sim 0$ (Fig. 6c). The model also predicted that N and P nutrient addition induced a transient shift from net autotrophy (GPP : CR > 1) to net heterotrophy (GPP : CR < 1) (Fig. 7c). In the model, shift toward net heterotrophy after dust seeding was partly attributed to the increase of the DOC : DOP ratio (Fig. 8f). The increase of the DOC : DOP ratio strengthened the C : P stoichiometric mismatch between DOM and

BGD
11, 2933–2971, 2014

bacteria, and enhanced postabsorptive, stoichiometrically regulated, respiration. All biological compartments also responded positively to nutrient addition; with an increase of the biomass from a minimum of +14 % for bacteria (for the scenario with $I_{C:P} < 0$, Fig. 8b), to a maximum of +70 % for chlorophyll *a*, ciliates and mesozooplankton (for the scenario with $I_{C:P} \sim 0$; Fig. 8a, c and e).

Predicted changes in chlorophyll biomass and PP were qualitatively consistent with observations from DUNE experiment. Observed chlorophyll *a* biomass increased from 111 ± 30 ng chl *a* L^{-1} to 220 ± 40 ng chl *a* L^{-1} (± SD) after nutrient addition, i.e. a relative change of +98 % (+50 % in the model, Fig. 8a). Measured PP increased from 4.57± 0.60 µg C L^{-1} d^{-1} to a maximum of 10.33 µg C l^{-1} d^{-1} (Guieu et al., 2014b; Ridame et al., 2014); in the model PP increased from 3.31 ± 0.77 µg C L^{-1} d^{-1} (Fig. 4) to a maximum of 10.88 µg C L^{-1} d^{-1} (Fig. 7). The increase in the DIN : DIP ratio after nutrient addition (Fig. 5c) was also consistent, though less pronounced, with the observed increase of the DIN : DIP ratio during DUNE experiments (Ridame et al., 2014). Predicted respiration rates after nutrient addition were however significantly lower (Fig. 7b) than those measured by Guieu et al. (2014b). In turn, the predicted net heterotrophy of the system after nutrient addition (Fig. 7c) was also lower than that observed during DUNE experiments.

4 Discussion

The question of how nutrient input from dust events influence microbial food web dynamics and carbon fluxes in the Mediterranean Sea was investigated during the DUNE experiments (Guieu et al., 2014a). In all experiments, the water masses enclosed in mesocosms were typically oligotrophic. The simulated dust depositions induced a transient increase of DIP and DIN concentrations, which, in turn, stimulated a response of the microbial food web to various degrees (Giovagnetti et al., 2013; Pulido-Vilena et al., 2010, 2014; Ridame et al., 2014; Guieu et al., 2014b). Measurements of Net Primary Production (NPP) and Bacterial Respiration (BR) from in vitro incubations revealed that

BGD
11, 2933–2971, 2014

the NPP : BR ratios were usually < 1.0, in both control and dust experiments, "*indicating that the total carbon processed by bacteria exceeds by far the carbon fixed by phytoplankton*" (Guieu et al., 2014b). As noted by Guieu et al. (2014b), these results were in agreement with the hypothesis that respiration can exceed planktonic photosynthesis in nutrient-depleted oligotrophic areas (Del Giorgio et al., 1997). However a controversy still exists on the real trophic status of the open ocean (i.e. net autotrophy vs. net heterotrophy), and questions remain about the mechanisms necessary to sustain high bacterial respiration rates in the ocean (Williams, 1998; Williams et al., 2013; Duarte et al., 2013).

The food web model described herein shed light on how ecological stoichiometry principles can influence the response of the microbial food web to dust deposition and the resulting trophic status of the ecosystem. Defining an index of C : P and C : N stoichiometric mismatch, the model suggested that C : N : P imbalance in food compare with consumer's requirement contributed to drive the balance between net autotrophy and net heterotrophy. Additionally, simulated nutrient input from dust can induce a transient shift from net autotrophy to net heterotrophy in five distinct scenarios which only differed by the strength of the stoichimetric mismatch between producers and consumers.

In the model, net heterotrophy was predicted when GPP was compared with total community respiration (CR), but not when GPP was compared with BR only (in this case, the predicted GPP : BR ratios were always > 1, not shown). Net heterotrophy (GPP : CR < 1) was predicted when food presented an excess of carbon compared to consumer requirements ($I_{C:P}$ and $I_{C:N} > 0$), leading to postabsorptive, stoichiometrically regulated, release of carbon (respired as CO_2 or excreted as L_{DOC}) in order to maintain consumer homeostasis. In the model, the parameterisation of postabsorptive release of C, N and P was inspired from previous studies addressing the fate of excess nutrient in consumers in pairwise predator–prey interactions (e.g. Sterner and Elser, 2002; Anderson et al., 2005). Several works have emphasized the role of bacterial decomposers in driving nutrient recycling (Anderson and Williams, 1998; Daufresne and

BGD
11, 2933–2971, 2014

Loreau, 2001; Cherif and Loreau, 2008). The model presented herein also extended ecological stoichiometry principles to a system comprising seven different resource-consumer interactions, including bacteria (Fig. 1). Model results also highlighted the role of bacteria on postabsorptive release of C, N and P in microbial food webs. First, primary production was strongly correlated to DIP excretion; with up to 34 % of P excretion being accounted for by the release of DIP from bacteria. Second, the predicted net heterotrophy (GPP : CR ratio < 1) was significantly correlated to C : N : P imbalance in dissolved organic matter (DOM) compared to bacterial requirement; with bacteria contributing to 41–54 % of the total postabsorptive respiration of the community.

In the model, regulation of postabsorptive bacterial respiration was entirely driven by carbon excess in DOM compared to bacterial requirement. The production of DOM with high C : P and C : N ratios was notably due to the production and released of L_{DOC} from phytoplankton under nutrient-limited conditions (parameter δ_p, Table 2). Production and excretion of DOC by phytoplankton under nutrient-limited conditions is one of the mechanisms that has been putted forward to explain the persistence of a significant drawdown of Dissolved Inorganic Carbon (DIC) concentrations in oligotrophic surface waters, despite severe nutrient-depletion (Sambrotto et al., 1993; Bates et al., 1996; Anderson and Pondaven, 2003).

However, although the model accounted for a parameterisation of DOC release from phytoplankton, this was not sufficient to drive the system to a state where NPP : BR ratios < 1; as observed during the DUNE experiments. Several reasons may explain this discrepancy.

First, model parameterisations of respiration and excretion rates were admittedly simple. Respiration rates were controlled by two parameters: (1) a maximal GGE ($\omega_B = 0.30$, and $a_i^{max} = 0.75$, Table 2), which accounted for various processes relating to maintenance, and (2) a mass balance approach maintaining homeostasis of the elemental composition in consumers. In reality, heterotrophic respiration includes – in addition to stoichiometrically regulated C release – various processes such as osmoregulation, biomass turnover, costs of somatic growth and reproduction, swim-

BGD
11, 2933–2971, 2014

ming, etc. Environmental constrains, food quantity or food quality can regulate the relative contribution of these processes to the total respiration for an organism (Anderson et al., 2005). A set of model frameworks which can scope with these various mechanisms exist, yielding to more realistic predictions of respiration rates over a wide range of environmental conditions (Anderson et al., 2005). However, we hypothesised that a more realistic parameterisation of respiration processes would not drive the system toward NPP : BR ratios << 1; notably because, in the model described herein, these processes are implicitly accounted for using the maximal GGE. For bacteria for example, the maximum GGE of $\omega_B = 0.30$ implied that 70 % of carbon intake is eventually respired.

Another reason for this discrepancy between the predicted and the observed net heterotrophy of the system could be a pool of preformed semi-labile DOC available in the mesocosms during the DUNE experiments; pool which would have sustained high BR. The model described here did not consider a semi-labile pool of DOC. To obtain such NPP : BR ratios < 1, this would require to increase the concentration of bioavailable DOC in the model by a factor of ~ 10 (i.e. a concentration of $L_{DOC} = \sim 10$–20 µM). Such values are consistent with observed concentrations of (labile + semi-labile) DOC in the western Mediterranean Sea (23.3 ± 2.7 µM; Aminot and Kerhouel, 2004).

The discrepancy between observation and model could also be attributed to an overestimation of BR due to methodological artefacts as it was highlighted in several recent papers (see for ex. Aranguren-Gassis et al., 2012). Guieu et al. (2014b), also argued that BR during DUNE-P could have been overestimated as BR values for the whole mesocosm was extrapolated from the rate measured at the depth of 5 m, meaning that BR was not homogeneous over the depth of the mesocosm contrary to what they hypothesized.

In conclusion, the simple food web model described herein has shed light on how ecological stoichiometric mismatch coupled with homeostatic regulation of C : N : P elemental composition in heterotrophic consumers can result in differential postabsorptive

BGD
11, 2933–2971, 2014

respiration and excretion of C, N, and P. All other things being equals, this mechanism can drive the system to net heterotrophy. In the model, net heterotrophy was notably driven by the production and excretion of extra DOC from phytoplankton under nutrient-limited conditions, which leaded to high C : P and C : N ratios of the DOM pool, and postabsorptive respiration of C by bacteria. The model also predicted that nutrient inputs from dust can result in a transient shift of the system from net autotrophy to net heterotrophy. However, the model was not able to account for the low NPP : BR ratios recorded during the DUNE experiments. A more realistic parameterisation of respiration rates in both autotrophic (e.g. Pahlow et al., 2013) and heterotrophic organisms (e.g. Anderson et al., 2005) could contribute to improve prediction of consistent NPP : BR ratios. May be more importantly, a better parameterisation of the sources and sinks of DOC at the surface of the ocean are needed (e.g. Anderson and Williams, 1999) such as the viral lysis, a process that can fuel back important amount of DOC in oligotrophic systems (Agusti and Duarte, 2013).

Supplementary material related to this article is available online at http://www.biogeosciences-discuss.net/11/2933/2014/bgd-11-2933-2014-supplement.pdf.

Acknowledgements. "The DUNE project, a DUst experiment in a low Nutrient, low chlorophyll Ecosystem, is a fundamental research project funded by the ANR under the contract" ANR-07-BLAN-0126-01. DUNE was endorsed by the international SOLAS (Surface Ocean – Lower Atmosphere) program in February 2009, (http://www.solas-int.org/activities/project-endorsement.html). P.P. was also supported by the LABEX-Mer (http://www.labexmer.eu/fr).

References

Agustí, S. and Duarte, C. M.: Phytoplankton lysis predicts dissolved organic carbon release in marine plankton communities, Biogeosciences, 10, 1259–1264, doi:10.5194/bg-10-1259-2013, 2013.

BGD
11, 2933–2971, 2014

Aminot, A. and Kérouel R.: Dissolved organic carbon, nitrogen and phosphorus in the N-E Atlantic and the N-W Mediterranean with particular reference to non-refractory fractions and degradation, Deep-Sea Res. Pt. I, 51, 1975–1999, 2004.
Anderson, T. R. and Pondaven, P.: Non-redfield carbon and nitrogen cycling in the Sargasso Sea: pelagic imbalances and export flux, Deep-Sea Res. Pt. I, 50, 573–591, 2003.
Anderson, T. R. and Williams, P. J.: Modelling the seasonal cycle of dissolved organic carbon at Station E1 in the English Channel, Est. Coast. Shelf Sci., 46, 93–109, 1998.
Anderson, T. R. and Williams, P. J.: A one-dimensional model of dissolved organic carbon cycling in the water column incorporating combined biological-photochemical decomposition, Global Biogeochem. Cy., 13, 13337–13349, doi:10.1029/1999GB900013, 1999.
Anderson, T. R., Hessen, D. O., Elser, J. J., and Urabe, J.: Metabolic stoichiometry and the fate of excess carbon and nutrients in consumers, Am. Nat., 165, 1–15, 2005.
Aranguren-Gassis, M., Teira, E., Serret, P., Martínez-García, S., and Fernández, E.: Potential overestimation of bacterial respiration rates in oligotrophic plankton communities, Mar. Ecol.-Prog. Ser., 453, 1–10, 2012.
Bates, N. R., Michaels, A. F., Knap, A. H.: Seasonal and interannual variability of oceanic carbon dioxide species at the US JGOFS Bermuda Atlantic Time-series Study (BATS) site, Deep-Sea Res. Pt. II, 43, 347–383, 1996.
Bergametti, G., Remoudaki, E., Losno, R., Steiner, E., and Chatenet, B.: Source, transport and deposition of atmospheric phosphorus over the northwestern Mediterranean, J. Atmos. Chem., 14, 501–513, doi:10.1007/BF00115254, 1992.
Boersma, M., Aberle, N., Hantzsche, F. M., Schoo, K. L., Wiltshire, K. H., and Malzahn, A. M.: Nutritional Limitation Travels up the Food Chain, Int. Rev. Hydrobiol., 93, 479–488, doi:10.1002/iroh.200811066, 2008.
Bonnet, S., Guieu, C., Chiaverini, J., Joséphine Ras, J., and Agnès Stock, A.: Impact of atmospheric inputs on the autotrophic communities in a low nutrient low chlorophyll system, Limnol. Oceanogr., 50, 1810–1819, 2005.
Calbet, A.: Mesozooplankton grazing effect on primary production: a global comparative analysis in marine ecosystems, Limnol. Oceanogr., 46, 1824–1830, 2001.
Cherif, M. and Loreau, M.: When microbes and consumers determine the limiting nutrient of autotrophs: a theoretical analysis, Proc. R. Soc. B, 276, 487–497, 2009.
Danger, M., Oumarou, C., Benest, D., and Lacroix, G.: Bacteria can control stoichiometry and nutrient limitation of phytoplankton, Funct. Ecol., 21, 202–210, 2007.

BGD
11, 2933–2971, 2014

Daufresne, T. and Loreau, M.: Plant-herbivore interactions and ecological stoichiometry: when do herbivores determine plant nutrient limitation, Ecol. Lett., 4, 196–206, 2001.
Del Giorgio, P. A., Cole, J. J., and Cimbleris, A.: Respiration rates in bacteria exceed phytoplankton production in unproductive aquatic systems, Nature, 385, 148–151, 1997.
Duarte, C. M., Regaudie-de-Gioux, A., Arrieta, J. M., Delgado-Huertas, A., and Agusti, S.: The oligotrophic ocean is heterotrophic, Annu. Rev. Mar. Sci., 5, 551–69, 2013.
Giovagnetti, V., Brunet, C., Conversano, F., Tramontano, F., Obernosterer, I., Ridame, C., and Guieu, C.: Assessing the role of dust deposition on phytoplankton ecophysiology and succession in a low-nutrient low-chlorophyll ecosystem: a mesocosm experiment in the Mediterranean Sea, Biogeosciences, 10, 2973–2991, doi:10.5194/bg-10-2973-2013, 2013.
Gismervik, I. and Andersen, T.: Prey switching by *Acartia clausi*: experimental evidence and implications of intraguild predation assessed by a model, Mar. Ecol.-Prog. Ser., 157, 247–259, 1997.
Guieu, C., Dulac, F., Desboeufs, K., Wagener, T., Pulido-Villena, E., Grisoni, J.-M., Louis, F., Ridame, C., Blain, S., Brunet, C., Bon Nguyen, E., Tran, S., Labiadh, M., and Dominici, J.-M.: Large clean mesocosms and simulated dust deposition: a new methodology to investigate responses of marine oligotrophic ecosystems to atmospheric inputs, Biogeosciences, 7, 2765–2784, doi:10.5194/bg-7-2765-2010, 2010.
Guieu, C., Dulac, F., Ridame, C., and Pondaven, P.: Introduction to project DUNE, a DUst experiment in a low Nutrient, low chlorophyll Ecosystem, Biogeosciences, 11, 425–442, doi:10.5194/bg-11-425-2014, 2014a.
Guieu, C., Ridame, C., Pulido-Villena, E., Blain, S., Bressac, M., Desboeufs, K., Dulac, F.: Dust deposition over oligotrophic marine environment: impact on carbon budget, Biogeosci., DUNE Special Issue, submitted, 2014b.
Herut, B., Zohary, T., Krom, M. D., Mantoura, R. F. C., Pitta, P., Psarra, S., Rassoulzadegan, F., Tanaka, T., and Thingstad, T. F.: Response of East Mediterranean surface water to Saharan dust: on-board microcosm experiment and field observations, Deep-Sea Res. Pt. II, 52, 3024–3040, 2005.
Hjerne, O. and Hansson, S.: The role of fish and fisheries in Baltic Sea nutrient dynamics, Limnol. Oceanogr., 47, 1023–1032, 2002.
Landry, M. R. and Calbet, A.: Microzooplankton production in the oceans, ICES J. Mar. Sci., 61, 501–507, 2004.

BGD
11, 2933–2971, 2014

Le Borgne, R.: Zooplankton production in the Eastern Tropical Atlantic Ocean: net growth efficiency and P : B in terms of carbon, nitrogen, and phosphorus, Limnol. Oceanogr., 27, 681–698, 1982.
Makino, W. and Cotner, J. B.: Elemental stoichiometry of a heterotrophic bacterial community in a freshwater lake: implications for growth- and resource-dependent variations, Aquat. Microb. Ecol., 34, 33–41, 2004.
Marañón, E., Fernández, A., Mouriño-Carballido, B., Martínez-García, S., Teira, E., Cermeño, P., Chouciño, P., Huete-Ortega, M., Fernández, E., Calvo-Díaz, A., Morán, X. A. G., Bode, A., Moreno-Ostos, E., Varela, M. M., Patey, M. D., and Achterberg, E. P.: Degree of oligotrophy controls the response of microbial plankton to Saharan dust, Limnol. Oceanogr., 55, 2339–2352, 2010.
Nugraha, A., Pondaven, P., and Tréguer, P.: Influence of consumer-driven nutrient recycling on primary production and the distribution of N and P in the ocean, Biogeosciences, 7, 1285–1305, doi:10.5194/bg-7-1285-2010, 2010.
Pahlow, M., Dietze, H., and Oschlies, A.: Optimality-based model of phytoplankton growth and diazotrophy, Mar. Ecol.-Prog. Ser., 489, 1–16, doi:10.3354/meps10449, 2013.
Pinhassi, J., Gomez-Consarnau, L., Alonso-Saez, L., Sala, M., Vidal, M., Pedrós-Alió, C., and Gasol, J. M.: Seasonal changes in bacterioplankton nutrient limitation and their effects on bacterial community composition in the NW Mediterranean Sea, Aquat. Microb. Ecol., 44, 241–252, 2006.
Pitt, K. A., Welsh, D. T., and Condon, R. H.: Influence of jellyfish blooms on carbon, nitrogen and phosphorus cycling and plankton production, Hydrobiol., 616, 133–149, 2009.
Price, N. M., Ahner, B. A., and Morel, F. M. M.: The equatorial Pacific Ocean: Grazer-controlled phytoplankton populations in an iron-limited ecosystem, Limnol. Oceanogr., 39, 520–534, 1994.
Pulido-Villena, E., Rérolle, V., and Guieu, C.: Transient fertilizing effect of dust in P-deficient LNLC surface ocean, Geophys. Res. Lett., 37, L01603, doi:10.1029/2009GL041415, 2010.
Redfield, A. C., Ketchum, B. H., and Richards, F. A.: The influence of organisms on the composition of sea-water, in: The Sea, vol. 2., edited by: Hill, M. N., Interscience Publishers, New York, 26–77, 1963.
Ridame, C., Guieu, C., and L'Helguen, S.: Strong stimulation of N_2 fixation in oligotrophic Mediterranean Sea: results from dust addition in large in situ mesocosms, Biogeosciences, 10, 7333–7346, doi:10.5194/bg-10-7333-2013, 2013.

BGD
11, 2933–2971, 2014

Ridame, C. Dekaezemacker, J., Guieu, C., B onnet, S., L'Helguen, S. and Malien, F.: Phytoplanktonic response to contrasted Saharan dust deposition events during mesocosm experiments in LNLC environment Biogeosciences Discuss., 11, 753–796, 2014, http://www.biogeosciences-discuss.net/11/753/2014/.
Sambrotto, R. N., Savidge, G., Robinson, C., Boyd, P., Takahashi, T., Karl, D. M., Landgon, C., Chipman, D., Marra, J., and Codispoti, C.: Elevated consumption of carbon relative to nitrogen in the surface ocean, Nature, 363, 248–250, 1993.
Siokou-Frangou, I., Christaki, U., Mazzocchi, M. G., Montresor, M., Ribera d'Alcalá, M., Vaqué, D., and Zingone, A.: Plankton in the open Mediterranean Sea: a review, Biogeosciences, 7, 1543–1586, doi:10.5194/bg-7-1543-2010, 2010.
Steinberg, D. K. and Saba, G. K.: Nitrogen consumption and metabolism in marine zooplankton, in: Nitrogen in the marine environment, 2 ed., edited by: Capone, D. G., Bronk, D. A., Mulholland, M. R., and Carpenter, E. J., Academic Press, Boston, MA, 1135–1196, 2008.
Sterner, R. W.: The ratio of nitrogen to phosphorus resupplied by herbivores: zooplankton and the algal competitive arena, Am. Nat., 136, 209–229, 1990.
Sterner, R. W. and Elser, J. J.: Ecological stoichiometry: the biology of elements from molecules to the biosphere, Princeton University Press, Princeton, 2002.
Straile, D.: Gross growth efficiencies of protozoan and metazoan zooplankton and their dependence on food concentration, predator-prey weight ratio, and taxonomic group, Limnol. Oceanogr., 42, 1375–1385, 1997.
Tanaka, T., Thingstad, T. F., Christaki, U., Colombet, J., Cornet-Barthaux, V., Courties, C., Grattepanche, J.-D., Lagaria, A., Nedoma, J., Oriol, L., Psarra, S., Pujo-Pay, M., and Van Wambeke, F.: Lack of P-limitation of phytoplankton and heterotrophic prokaryotes in surface waters of three anticyclonic eddies in the stratified Mediterranean Sea, Biogeosciences, 8, 525–538, doi:10.5194/bg-8-525-2011, 2011.
Ternon, E., Guieu, C., Ridame, C., L'Helguen, S., and Catala, P.: Longitudinal variability of the biogeochemical role of Mediterranean aerosols in the Mediterranean Sea, Biogeosciences, 8, 1067–1080, doi:10.5194/bg-8-1067-2011, 2011.
Thingstad, T. F., Zweifel, U. L., and Rassoulzadegan, F.: P limitation of heterotrophic bacteria and phytoplankton in the northwest Mediterranean, Limnol. Oceanogr., 43, 88–94, 1998.
Thingstad, F. T., Krom, M. D., Mantoura, R. F. C., Flaten, G., Groom, S., Herut, B., Kress, N., Law, C. S., Pasternak, A., Pitta, P., Psarra, S., Rassoulzadegan, F., Tanaka, T., Tselepides, A., Wassmann, P., Woodward, E. M. S., Wexels-Riser, C., Zodiatis, G., and Zohary, T.:

BGD
11, 2933–2971, 2014

Nature of phosphorus limitation in the ultra-oligotrophic Eastern Mediterranean, Science, 309, 1068–1071, 2005.

Timmermans, K. R., van der Wagt, B., and Hein, J. W., and de Baar, H. J. W.: Growth rates, half-saturation constants, and silicate, nitrate, and phosphate depletion in relation to iron availability of four large, open-ocean diatoms from the Southern Ocean, Limnol. Oceanogr., 49, 2141–2151, 2004.

Touratier, F., Field, J. G., and Moloney, C. L.: A stoichiometric model relating growth substrate quality (C : N : P ratios) to N : P ratios in the products of heterotrophic release and excretion, Ecol. Model., 139, 265–291, 2001.

Vadstein, O., Andersen, T., Reinertsen, H. R., and Olsen, Y.: Carbon, nitrogen and phosphorus resource supply for coastal planktonic heterotrophic bacteria in a gradient of nutrient loading, Mar. Ecol.-Prog. Ser., 447, 55–75, 2012.

The balance of plankton respiration and photosynthesis in the open oceans, Nature, 394, 55–57, 1998.

Williams, P. J., Quay, P. D., Westberry, T. K., and Behrenfeld, M. J.: The oligotrophic ocean is autotrophic, Annu. Rev. Mar. Sci., 5, 535–49, 2013.

Wuttig, K., Wagener, T., Bressac, M., Dammshäuser, A., Streu, P., Guieu, C., and Croot, P. L.: Impacts of dust deposition on dissolved trace metal concentrations (Mn, Al and Fe) during a mesocosm experiment, Biogeosciences, 10, 2583–2600, doi:10.5194/bg-10-2583-2013, 2013.

Zohary, T., Herut, B., Krom, M. D., Fauzi, R., Mantoura, C., Pitta, P., Psarra, S., Rassoulzadegan, F., Stambler, N., Tanaka, T., Thingstad, T. F., Malcolm, E., and Woodward, E.: P-limited bacteria but N and P co-limited phytoplankton in the Eastern Mediterranean – a microcosm experiment, Deep-Sea Res. Pt. II, 52, 3011–3023, doi:10.1016/j.dsr2.2005.08.011, 2005.

BGD
11, 2933–2971, 2014

Table 1. Model equations.

$$\frac{dB_P}{dt} = U_B^{DOP} + U_B^{DIP} - E_B^P - l_B^H H_P$$

$$\frac{dA_P}{dt} = U_A A_P - l_A^H H_P$$

$$\frac{dD_P}{dt} = U_D D_P - l_D^C C_p - l_D^M M_P$$

$$\frac{dH_P}{dt} = \left(a_P^{BH} l_B^H + a_P^{AH} l_A^H\right) H_P - l_H^C C_P$$

$$\frac{dC_P}{dt} = \left(a_P^{HC} l_H^C + a_P^{DC} l_D^C\right) C_p - l_C^M M_P$$

$$\frac{dM_P}{dt} = \left(a_P^{DM} l_D^M + a_P^{CM} l_C^M\right) M_P - \delta_M M_P$$

$$\frac{dP_i}{dt} = \lambda_e \left(\begin{array}{l} \left[\left(1 - a_P^{BH}\right) l_B^H + \left(1 - a_P^{aH}\right) l_A^H\right] H_P \\ + \left[\left(1 - a_P^{HC}\right) l_H^C + \left(1 - a_P^{DC}\right) l_D^C\right] C_P \\ + \left[\left(1 - a_P^{DM}\right) l_D^M + \left(1 - a_P^{CM}\right) l_C^M\right] M_P + \delta_M M_P \end{array} \right) + E_B^P - U_B^{DIP} - U_A A_p - U_d D_p + E_{P_i}$$

$$\frac{dL_{DOP}}{dt} = (1 - \lambda_e) \left(\begin{array}{l} \left[\left(1 - a_P^{BH}\right) l_B^H + \left(1 - a_P^{AH}\right) l_A^H\right] H_p \\ + \left[\left(1 - a_P^{HC}\right) l_H^C + \left(1 - a_P^{DC}\right) l_D^C\right] C_p \\ + \left[\left(1 - a_P^{DM}\right) l_D^M + \left(1 - a_P^{CM}\right) l_C^M\right] M_p + \delta M_P \end{array} \right) - U_B^{DOP}$$

$$\frac{dN_i}{dt} = \lambda_e \left(\begin{array}{l} \left[\theta_B^{NP}\left(1 - a_N^{BH}\right) l_B^H + \theta_A^{NP}\left(1 - a_N^{AH}\right) l_A^H\right] H_p \\ + \left[\theta_H^{NP}\left(1 - a_N^{HC}\right) l_H^C + \theta_D^{NP}\left(1 - a_N^{DC}\right) l_D^C\right] C_P \\ + \left[\theta_D^{NP}\left(1 - a_N^{DM}\right) l_D^M + \theta_C^{NP}\left(1 - a_N^{CM}\right) l_C^M\right] M_p + \theta_M^{NP}\delta_M M_P \end{array} \right) + E_B^N - U_B^{DIN} - \theta_A^{NP} U_A A_p - \theta_D^{NP} U_d D_p + E_{N_i}$$

$$\frac{dL_{DON}}{dt} = (1 - \lambda_e) \left(\begin{array}{l} \left[\theta_B^{NP}\left(1 - a_N^{BH}\right) l_B^H + \theta_A^{NP}\left(1 - a_N^{AH}\right) l_A^H\right] H_p \\ + \left[\theta_H^{NP}\left(1 - a_N^{HC}\right) l_H^C + \theta_D^{NP}\left(1 - a_N^{DC}\right) l_D^C\right] C_P \\ + \left[\theta_D^{NP}\left(1 - a_N^{DM}\right) l_D^M + \theta_C^{NP}\left(1 - a_N^{CM}\right) l_C^M\right] M_p + \theta_M^{NP}\delta_M M_P \end{array} \right) - U_B^{DON}$$

$$\frac{dL_{DOC}}{dt} = (1 - \lambda_e) \left(\begin{array}{l} \left[\theta_B^{CP}\left(1 - a_C^{BH}\right) l_B^H + \theta_A^{CP}\left(1 - a_C^{AH}\right) l_A^H\right] H_P \\ + \left[\theta_H^{CP}\left(1 - a_C^{HC}\right) l_H^C + \theta_D^{CP}\left(1 - a_C^{DC}\right) l_D^C\right] C_P \\ + \left[\theta_D^{CP}\left(1 - a_C^{DM}\right) l_D^M + \theta_C^{CP}\left(1 - a_C^{CM}\right) l_C^M\right] M_p + \theta_M^{CP}\delta_M M_P \end{array} \right) - U_B^{DOC} + E_P$$

BGD
11, 2933–2971, 2014

Table 2. Ecosystem model parameters.

Symbol	Parameter	Unit	Value
Bacteria			
μ_{max}^{B}	Maximum growth rates for bacteria	hr-1	0.25
$K_{P_i}^{B}, K_{N_i}^{B}, K_{LDOC}^{B}$	Bacteria half-saturation constants for growth on DIP, DIN and L_{DOC}	nM-P, nM-N, nM-C	50, 500, 20 000
$\theta_{B}^{NP}, \theta_{B}^{CP}$	N : P and C : P ratios for bacteria	mol mol^{-1}	see text
ω_B	Maximum carbon GGE for bacteria	dimensionless	0.30
Phytoplankton			
$\mu_{max}^{pico}, \mu_{max}^{nano}$	Maximum growth rates for autotrophic pico- and nanoplankton	h^{-1}	0.08, 0.10
$K_{P_i}^{Pico}, K_{P_i}^{nano}$	Autotrophic pico- and nanoplankton half-saturation constants for growth on DIP	nM-P	100, 200
$K_{N_i}^{Pico}, K_{N_i}^{nano}$	Autotrophic pico- and nanoplankton half-saturation constants for growth on DIN	nM-N	1000, 1800
$\theta_{A}^{NP}, \theta_{A}^{CP}$	N : P and C : P ratios for autotrophic picoplankton	mol mol^{-1}	see text
$\theta_{D}^{NP}, \theta_{D}^{CP}$	N : P and C : P ratios for autotrophic nanoplankton	mol mol^{-1}	see text
δ_P	Production of extra carbon from nutrient-lmited primary production	dimensionless	0.26
HNF, ciliates and mesozooplankton			
$g_{h}^{max}, g_{C}^{max}, g_{M}^{max}$	Maximum growth rates for HNF, ciliates and mesozooplankton	h^{-1}	0.07, 0.05, 0.02
C_{B}^{H}, C_{A}^{H}	Incipient limitation bacteria and picophytoplankton conc. for HNF	nM-P	30, 30
C_{D}^{C}, C_{H}^{C}	Incipient limitation nanophytoplankton and HNF conc. for ciliates	nM-P	40, 40
C_{D}^{M}, C_{C}^{M}	Incipient limitation nanophytoplankton and ciliates conc. for mesozooplankton	nM-P	40, 16
φ	Switching shape parameter	dimensionless	2.0
$\theta_{H}^{NP}, \theta_{H}^{CP}$	N : P and C : P ratios for HNF	mol mol^{-1}	See text
$\theta_{C}^{NP}, \theta_{C}^{CP}$	N : P and C : P ratios for ciliates	mol mol^{-1}	See text
$\theta_{M}^{NP}, \theta_{M}^{CP}$	N : P and C : P ratios for mesozooplankton	mol mol^{-1}	See text
a_{i}^{max}	Maximum GGE for HNF, ciliates and mesozooplankton	dimensionless	0.75
$a_{P}^{BH}, a_{N}^{BH}, a_{P}^{AH}, a_{N}^{AH}$	P and N GGE for HNF (H) feeding on bacteria (B) or autotrophic picoplankton (A)	dimensionless	calculated
$a_{P}^{DC}, a_{N}^{DC}, a_{P}^{HC}, a_{N}^{HC}$	P and N GGE for ciliates (C) feeding on autotrophic nanoplankton (D) and HNF (H)	dimensionless	calculated
$a_{P}^{DM}, a_{N}^{DM}, a_{P}^{CM}, a_{N}^{CM}$	P and N GGE for mesozooplankton (M) feeding on autotrophic nanoplankton (D) and ciliates (C)	dimensionless	calculated
δ_M	Mortality rate for mesozooplankton	h^{-1}	0.003
Other processes			
λ_e	Fraction of postabsorptive excretion released as dissolved inorganic nutrients or CO_2	dimensionless	0.60

BGD
11, 2933–2971, 2014

Table 3. N : P and C : P elemental ratios of bacteria (Bp) picophytoplankton (Ap), nanophytoplanktyon (Dp), heterotrophic nanoflagellates (Hp), Ciliates (Cp) and mesozooplankton (Mp) for the five scenarios used to evaluate the influence of N and P inputs on food web dynamics. $I_{C:P}$: index of C : P stoichiometric mismatch (see text).

		N : P ratio (mol mol^{-1})						C : P ratio (mol mol^{-1})					
	$I^{*}_{C:P}$	Bp	Ap	Dp	Hp	Cp	Mp	Bp	Ap	Dp	Hp	Cp	Mp
IC : P < 0	−161.04	12.60	15.94	15.67	8.98	12.20	10.98	150.21	66.07	54.43	92.19	127.06	147.27
IC : P ∼ 0	−0.03	22.92	19.67	21.05	15.60	9.66	10.94	100.87	68.34	139.21	131.72	88.09	156.61
IC : P > 0	263.17	21.19	8.27	12.20	13.00	21.29	17.46	144.81	142.33	156.09	60.81	82.55	60.45
Redfield (1963)	62.00	16.00	16.00	16.00	16.00	16.00	16.00	106.00	106.00	106.00	106.00	106.00	106.00
Vadstein et al. (2012)	115.15	7.5	25.00	28.00	19.00	20.00	24.00	34.4	129.2	172.2	123.00	83.00	76.00

* mol C mol^{-1} P

BGD
11, 2933–2971, 2014

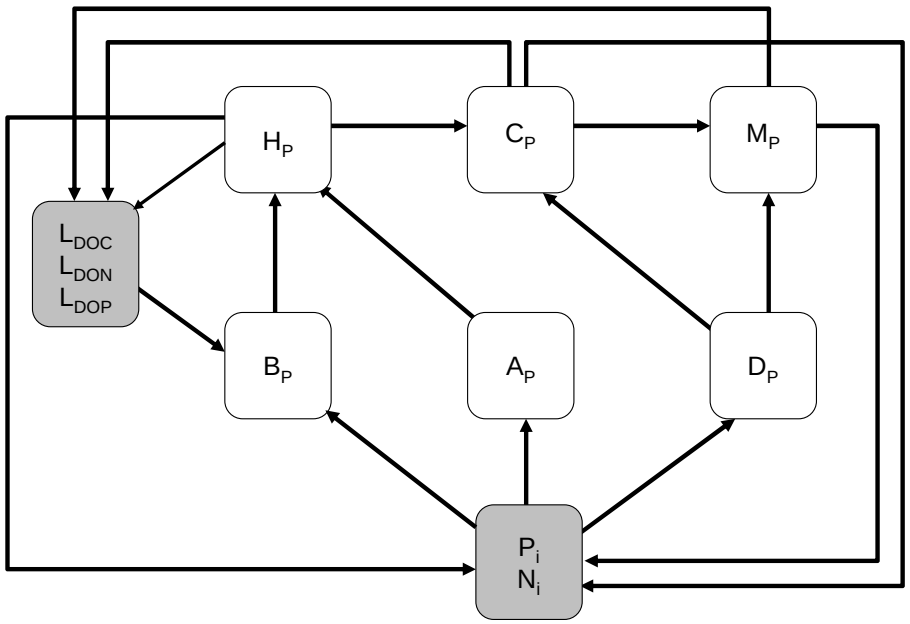

Fig. 1. Conceptual scheme of the food web model (adapted from Thingstad et al., 2007) showing state variables (white and grey boxes) and fluxes (arrows). The model included three osmotrophs, i.e. heterotrophic bacteria (B_P), and two phytoplankton types, autotrophic picoplankton (A_P) and nanoplankton (D_P). The growth rate of phytoplankton relied on the availability of dissolved inorganic nitrogen (N_i) and phosphorus (P_i). Bacterial growth primarily relied on the availability of dissolved organic matter (L_{DOM}), and secondarily on the availability of N_i and P_i. Three predators were included in the model: heterotrophic nanoflagellates (H_P), ciliates (C_P) and mesozooplankton (M_P). The subscript "P" indicates that the main model currency was phosphorus. It was assumed that all organisms had a fixed C : N : P elemental composition, so that explicit equations for N and C pools stored in organisms were not required (with the exception of the DOM pool).

BGD
11, 2933–2971, 2014

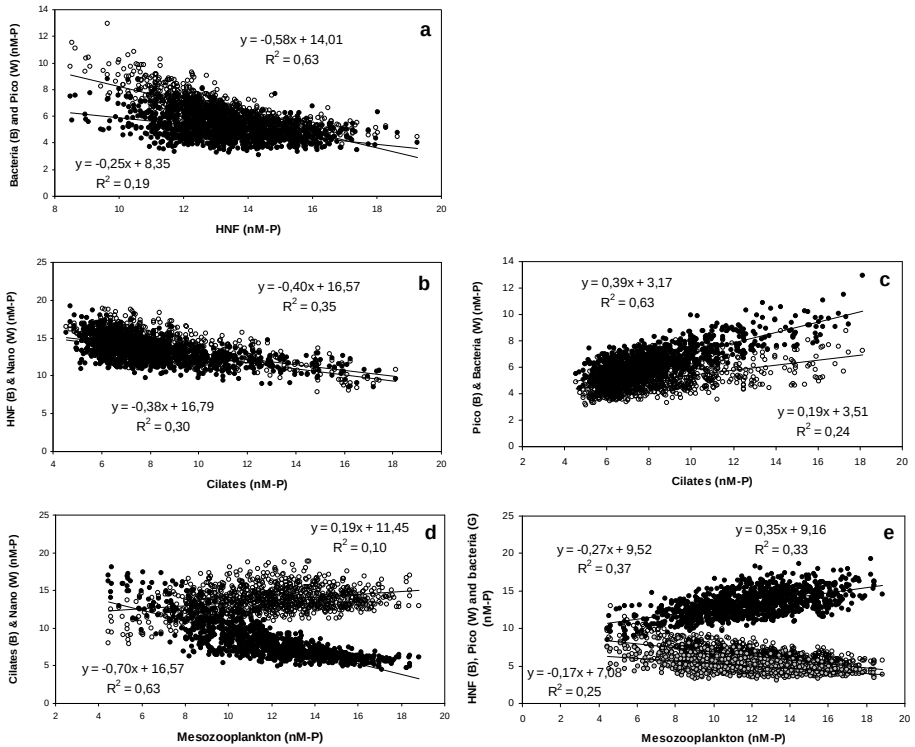

Fig. 2. Asymptotic model solutions (each point represented the steady state solution obtained at time $t = 4 \times 10^4$ h) from 1000 simulations wherein which the C : N : P elemental stoichiometry of each organism was chosen randomly in a range of ± 50 % around the Redfield ratio (C : N : P = 106 : 16 : 1; Redfield et al., 1963); the other model parameters were set to their default values given in Table 2. Results from linear regression are indicated (all p values were < 0.01). On the y-axis: B (black dots), W (white dots) and G (grey dots).

BGD
11, 2933–2971, 2014

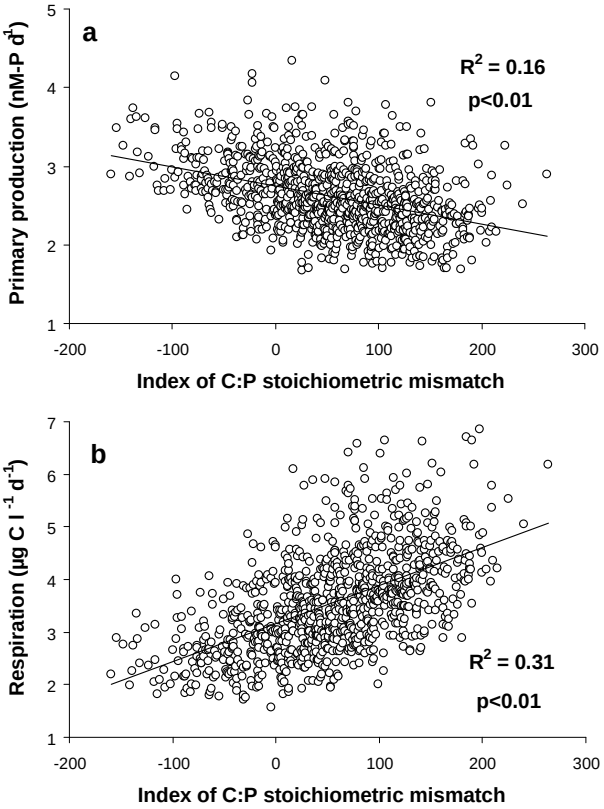

Fig. 3. Asymptotic model solutions (each point is the steady state solution obtained at time t = 4×10^4 h) from 1000 simulations, in which the C : N : P elemental stoichiometry of each organism was chosen randomly in a range of ± 50 % around the Redfield ratio (C : N : P = 106 : 16 : 1); the other model parameters were set to their default values given in Table 2; **(a)** primary production (nM-P d^{-1}) and **(b)** community respiration (µg C L^{-1} d^{-1}) plotted against the Index of C : P stoichiometric mismatch, $I_{C:P}$ (see text for details on the calculation of $I_{C:P}$).

BGD
11, 2933–2971, 2014

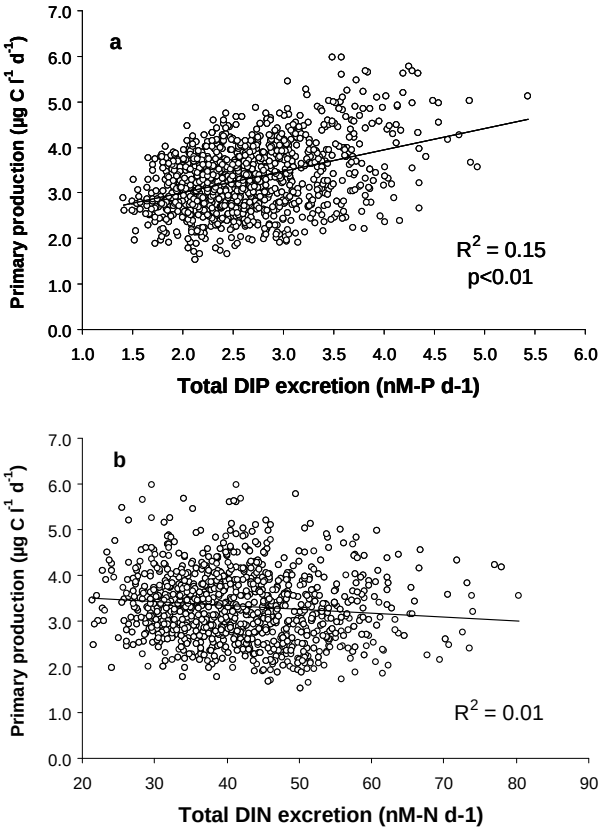

Fig. 4. Asymptotic model solutions (at $t = 4 \times 10^4$ h) from 1000 simulations in which the carbon, nitrogen and phosphorus elemental stoichiometry of each organism was chosen randomly in a range of ±50 % around the Redfield ratio; the other parameters were set to their default values given in Table 2; **(a)** Total DIP and **(b)** total DIN regeneration from bacteria, HNF, ciliates and mesozooplankton.

BGD
11, 2933–2971, 2014

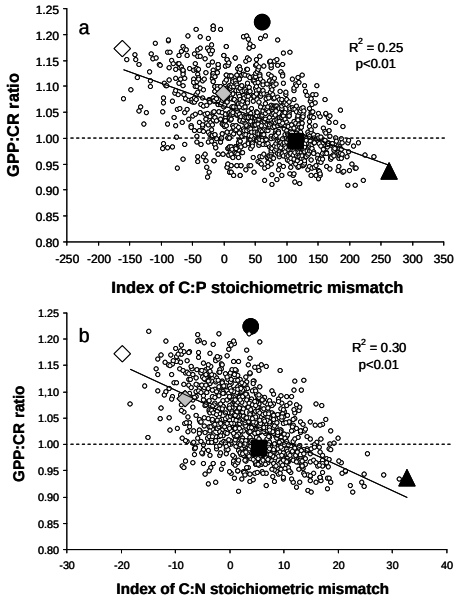

Fig. 5. Asymptotic model solutions from 1000 simulations (open circles; each point is the steady state solution obtained at time $t = 4 \times 10^4$ h), in which the C : N : P elemental stoichiometry of each organism was chosen randomly in a range of ± 50 % around the Redfield ratio (C : N : P = 106 : 16 : 1); the other model parameters were set to their default values given in Table 2; **(a)** GPP : CR ratio plotted against the Index of C : P stoichiometric mismatch, $I_{C:P}$, and **(b)** GPP : CR ratio plotted against the $I_{C:N}$ (see text for details on the calculation of $I_{C:P}$ and $I_{C:N}$). The asymptotic model solutions from 3 cases were subsequently used as initial conditions to evaluate the influence of nutrient input from dust (DUNE experiment) on food web dynamics (see text): $I_{C:P} \ll 0$ (◊), $I_{C:P} \sim 0$ (◈), and $I_{C:P} \gg 0$ (▲). Two additional cases were also treated: a simulation in which C : N : P ratios were from Redfield for all organisms (●), or with C : N : P ratios from Vadstein et al. (2012) (■).

BGD
11, 2933–2971, 2014

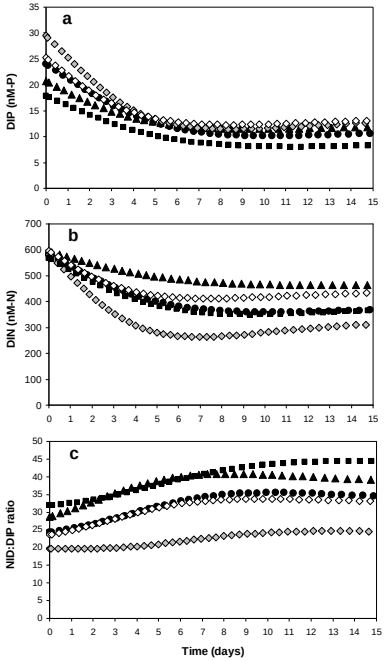

Fig. 6. Predicted **(a)** dissolved inorganic phosphorus (DIP), **(b)** dissolved inorganic nitrogen (DIN) and **(c)** DIP : DIN ratio over a period of 15 days after a nutrient input from dust at $t = 0$ (+4.30 nM-P and +498 nM-N; DUNE experiment, Ridame et al., 2014). $I_{C:P} \ll 0$ (◊), $I_{C:P} \sim 0$ (◆), and $I_{C:P} \gg 0$ (▲). Two additional cases were also treated: a simulation with C : N : P ratios following Redfield for all organisms (●), or with C : N : P ratios from Vadstein et al. (2012) (■). For each case, the initial conditions at $t = 0$ were steady the state solutions obtained after a simulation of 40 000 h, prior to nutrient addition.

BGD
11, 2933–2971, 2014

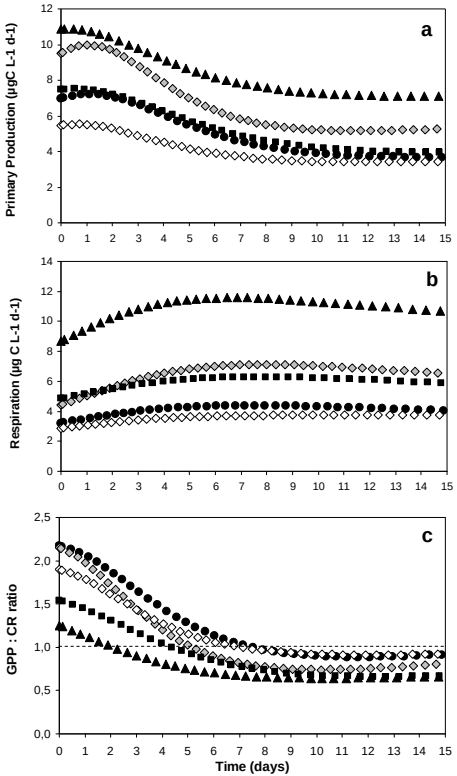

Fig. 7. Predicted **(a)** gross primary production (GPP), excluding production of dissolved organic carbon, **(b)** respiration of the whole community (CR) and **(c)** GPP : CR ratio over a period of 15 days after a nutrient addition at $t = 0$ (+4.30 nM-P and +498 nM-N; DUNE experiment "P", Guieu et al., 2014b). $I_{C:P} \ll 0$ (◊), $I_{C:P} \sim 0$ (◈), and $I_{C:P} \gg 0$ (▲). Two additional cases were also treated: a simulation with C : N : P ratios following Redfield for all organisms (●), or with C : N : P ratios from Vadstein et al. (2012) (■). For each case, the initial conditions at $t = 0$ were steady the state solutions obtained after a simulation of 40 000 h, prior to nutrient addition.

BGD
11, 2933–2971, 2014

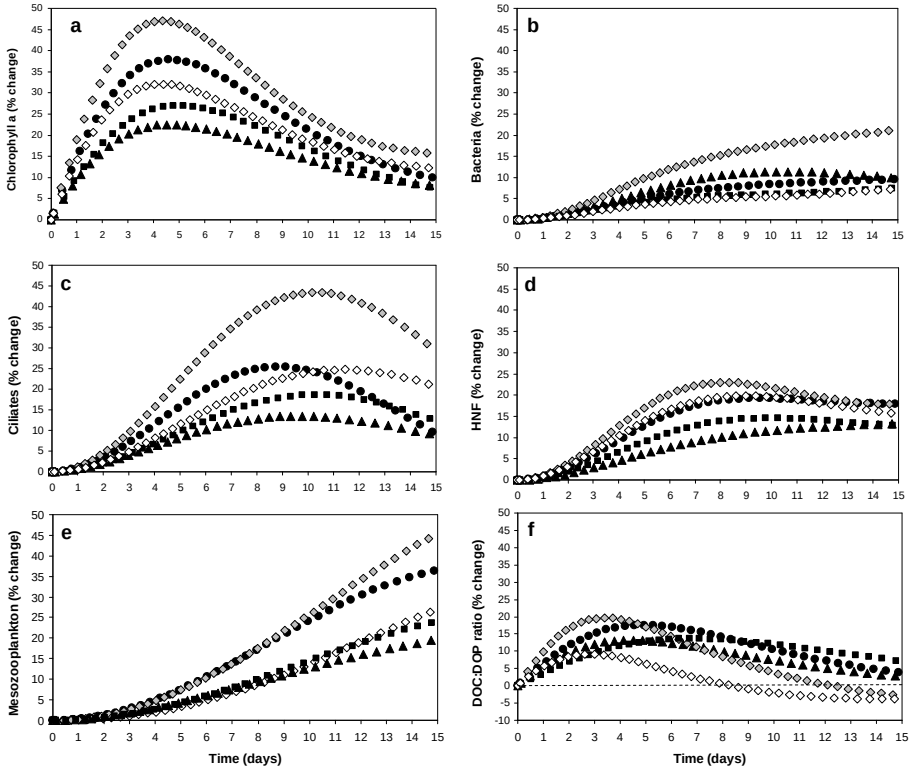

Fig. 8. Relative change after nutrient addition at $t = 0$ (+12.90 nM-P and +571.4 nM-N, DUNE experiment "P", Guieu et al., 2014b). **(a)** chlorophyll *a*, **(b)** Bacteria, **(c)** Ciliates, **(d)** HNF, **(e)** Mesozooplankton, and **(f)** DOC : DOP ratio; $I_{C:P} \ll 0$ (◊), $I_{C:P} \sim 0$ (◈), and $I_{C:P} \gg 0$). Two additional cases were also treated: a simulation with C : N : P ratios following Redfield for all organisms (●), or with C : N : P ratios from Vadstein et al. (2012) (■). For each case, the initial conditions at $t = 0$ were steady the state solutions obtained after a simulation of 40 000 h, prior to nutrient addition.

BGD
11, 2933–2971, 2014